**Strigolactones promote flowering by inducing the miR319-LA-SFT module in tomato**



*Published version:*

DOI:10.1073/pnas.2316371121

www.pnas.org

# Supplementary Information for

## Strigolactones promote flowering by inducing the miR319-*LA*-*SFT* module in tomato

Ivan Visentin, Leticia Frizzo Ferigolo, Giulia Russo, Paolo Korwin Krukowski, Caterina Capezzali, Danuše Tarkowská, Francesco Gresta, Eleonora Deva, Fabio Tebaldi Silveira Nogueira, Andrea Schubert, Francesca Cardinale*

*Francesca Cardinale, DISAFA PlantStressLab, largo P. Braccini 2, Grugliasco (TO), 10095 Italy. Phone number: +390116708875

**Email:** francesca.cardinale@unito.it

**This PDF file includes:**

Supplementary text

Figures S1 to S10

Tables S1 to S5

Legends for Datasets S1 to S3

SI References

**Other supplementary materials for this manuscript include the following:**

Datasets S1 to S3

## Supplementary text

## Results

### Strigolactone deficiency widely affects the transcription of genes in the flowering network

Besides the genes highlighted in the manuscript body, we found a down-regulation of several MADS-box transcription factors involved in tomato floral transition (Table S1, Dataset S2), namely the *FRUITFULL-like* genes *FUL1* and *FUL2* (40), *MADS-BOX PROTEIN13* (*MBP13*), *MBP14*, *MBP15*, *MBP18*/*FYFL*, *MBP20* and *MBP56* (54), *JOINTLESS* (*J*) (49), tomato B-class MADS-box gene *TM6*/*TDR6* and *AGAMOUS1* (*TAG1*) (48, 55). Three members of the *CONSTANS* (*CO*)/*CONSTANS-like* (*COL*) gene family, related to photoperiodic signaling and flowering in tomato (49), were found down-regulated (*CO1*, *CO3* and *COL4a*), while *COL* was slightly up-regulated. The transcription factor-encoding gene *NAP2* (*NUCLEOSOME ASSEMBLY PROTEIN2*) of the *NAC* (*NAM*, *No apical meristem*; *ATAF*; *CUC*, *Cup-shaped Cotyledon*) family, activated by Apetala3/Pistillata (AP3/PI), is strongly down-regulated ($log_2FC = -4.5$). This protein controls both leaf senescence and fruit yield in tomato, and *NAP2*-overexpressing plants start producing flowers around one week earlier than wt plants (56, 57). Three other genes encoding NAC-domain transcription factors, *NAM2* and *NAM3*, and the *NAM* homologue *GOBLET* (*GOB)*, involved in floral morphogenesis in tomato (57, 58), were also down-regulated in SL- plants. Other DEGs listed in Table S1 have not been functionally characterized in tomato yet, and have been mainly identified through bioinformatic (59) or transcriptome studies (60, 61) based on the role of their putative homologues in floral transition pathways of *A. thaliana* and other model plants. Among down-regulated genes we found the tomato orthologues of the genes coding for: MYB-related transcription factors LATE ELONGATED HYPOCOTYL (LHY) and CIRCADIAN CLOCK ASSOCIATED 1 (CCA1) (62); TIMING OF CAB EXPRESSION 1 (TOC1), a member of the PSEUDO-RESPONSE REGULATOR (PRR) family (59) that controls photoperiodic flowering response in *A. thaliana*, positively regulating *CCA1* and *LHY* expression (63); the Transducin/WD40 repeat-like superfamily protein COP1, an E3 ubiquitin-protein ligase that acts as a repressor of photomorphogenesis and is involved in the degradation of CO during the night (64, 65); the EARLY FLOWERING (ELF) 3 and ELF4, which function as modulators of light signal transduction downstream of phytochromes and control photoperiodic flowering by interacting with COP1 and regulating GIGANTEA (GI) stability (66, 67); and ELF7, a RNA polymerase II-associated factor Paf1 involved in the regulation of flowering time (68). On the other hand, among the most interesting up-regulated genes, we found the one encoding the circadian oscillator GI, involved in photoperiod-dependent floral transition in several plant species (69); and a putative orthologue of the AP2-like transcription factor-encoding *TARGET OF EAT1* (*TOE1*) named *AP2d* (70). Moreover, a set of genes encoding transcription factors belonging to the large Nuclear Factor Y (NF-Y) family, involved in flowering control (71), were found to be down-regulated in the SL- genotype.

Several genes in Table S1 are also related to DNA modifications and chromatin remodeling: the gene coding for the replication protein RPA1b is up-regulated (72, 73), while one for the MULTICOPY SUPRESSOR OF IRA1 (MSI1)-like chromatin-adaptor protein MSI1 (71) is down-regulated. Also, two genes encoding the DNA mismatch repair proteins MutS HOMOLOGS, MSH1 (74), and MSH2 (75), are up- and down-regulated, respectively. Three more uncharacterized gene products were identified in the GO enrichments process, all of which were found to be down-regulated in the SL- plants: the putative orthologue of the *A. thaliana BONSAI* (*BNS*), encoding an ubiquitin–protein ligase complex that regulates cell cycle progression (76); one encoding the cell wall-localized class III peroxidase PER17, the orthologue of which is involved in the transition to flowering and timing of lignified tissue formation in *A. thaliana* (77); and the one encoding a Snf1-related kinase-interacting protein (*SKI2*, similar to At1g80940), which is annotated as involved in the regulation of flower development based on InterPro classification.

## Materials and Methods

### Plant materials and growth conditions

The tomato *SlCCD7*-silenced line 6936, here called SL-, and its wt genotype M82 were a kind gift by Dr. H. J. Klee (University of Florida) (28) and show 70-80% reduction of strigolactone content in root tissues and exudates. The $LA_{pro}$>>$La^{m}$-*GFP* genotype (18) expresses *La-2*, a miR319-insensitive version of *LA* (78), under the control of the *LA* promoter and in translational fusion with GFP in the M82 background. Seeds were sterilized in 4% (v/v) sodium hypochlorite containing 0.02% (v/v) Tween 20, rinsed thoroughly with sterile water, and then placed for 48 h on moistened filter paper at 25°C in darkness. Plants were grown for two weeks in a walk-in climate chamber (16/8h light/dark 25°C) in a seedbed with standard soil (Terra Nature, NPK 12:14:24) and subsequently moved into 5-liter pots under greenhouse conditions. From the transplanting to the end of the experiments, plants were fertilized with a standard half-strength Hoagland solution twice a week. Plant age was counted starting at the emergence of cotyledons from the soil bed.

For the experiment described in fig. 2A and S3A, 4-day-old M82 wt plants were sprayed until runoff on the whole aerial part with a 5 μM solution of $GR24^{5DS}$ (synthetic strigolactone analogue from StrigoLab Srl, Turin, Italy) in 0.01% v/v acetone in water (n=6-13). Analogously, the control plants were sprayed with a corresponding acetone solution. Six days after the first treatment, when around 50% of the plants were at the transition stage, the plants were split in two groups: group 1 was not further treated (fig. S3A) while group 2 received an additional $GR24^{5DS}$ treatment (fig. 2A). The meristems were evaluated 4 to 12 days after the first treatment under the stereomicroscope and classified as vegetative meristem (VM), transition meristem (TM), inflorescence meristem (IM) or floral meristem (FM).

For the leaf-spraying experiment described in fig. 2B-E, 3-week-old wt plants grown under the same conditions mentioned above were sprayed with the same 5 μM solution of $GR24^{5DS}$ in 0.01% v/v acetone in water, or with a corresponding acetone solution (n=8). Ripening fruits (35) were counted until 80 days, and weighed until 92 days after the treatment. Leaves (about 100 mg fw) were collected as above 2, 6, and 24 hours after the treatment and stored at −80°C until analysis. For the leaf-spraying experiments described in fig. 3C-E, 8-day-old or 4-week-old wt and $LA_{pro}$>>$LA^{m}$-*GFP* plants were treated as above with $GR24^{5DS}$ (n=8). The number of leaves to the first inflorescence was counted at anthesis (*i.e.* stage 3 as defined earlier (34)). For the experiment in fig. 3A, 4-week-old wt plants were grown and treated as in the experiment in fig. 2B-E (n=5). For each plant, a sample consisting of three young leaves was collected 0, 15’, 1h, 6h and 24h after treatment. The samples were processed for gene transcript quantification as described below. For the experiment in fig. 4 and S5, vegetative wt plants were treated with 5 μM $GR24^{5DS}$ 8 days after seedling emergence, and harvested one week later; another subset was treated in the reproductive phase, 23 days after germination, and harvested at 30 days. Each treatment had n=6 (each sample the pool of 10 individual meristems).

For the grafting experiment described in fig. 1, 3B, S2A-B, three grafted lines were produced by the clamp-grafting technique on plants at the 2/4-leaf stage (about 3 weeks after seedling emergence) and with a stem diameter of 1.5–2 mm (n=5; wt or SL- rootstock and scion, wt/wt or SL-/SL-, respectively; and wt scion grafted to a SL- rootstock, wt/SL-). After 3 additional weeks of acclimation, grafted plants were transplanted and grown in the greenhouse as above. The daily count of new individual flowers at anthesis started 3 weeks after graft production (*i.e.* at transplant) and continued for 3 weeks. A subset of self-grafted wt/wt plants were treated 1 and 3 weeks after grafting with 5 μM $GR24^{5DS}$. Ripening fruits (35) were counted and weighed 60 days after grafting. For gene transcript quantification, leaves of comparable physiological stage (about 100 mg fw) were collected 20 days after grafting from each plant, deep-frozen, and stored at −80°C until analysis.

For transcriptome analysis, at least 3 fully expanded leaves were collected (one per plant) from 5 wt and SL- plants, grown for 3 weeks after seedling emergence in a walk-in climate chamber set at 16/8h light/dark 25°C. Leaves were collected at 9.00 am, 3 h into the light period.

**Library construction, sequencing, and processing of mRNA data**

Total RNA was extracted from 3-week-old wt and SL- tomato leaves using the Spectrum Plant Total RNA Kit (Sigma Aldrich). After digestion of contaminant DNA by DNAse I (ThermoScientific) at 37°C for 30 min, RNA quantity and quality were determined with a Nanodrop 2000 spectrophotometer (Thermo Fisher Scientific Inc., Wilmington, DE, United States) and sent to Novogene Europe for library construction and sequencing (Cambridge, United Kingdom). There, RNA degradation and contamination were monitored on 1% agarose gels, RNA purity was checked using the NanoPhotometer® spectrophotometer (IMPLEN, CA, USA), and RNA integrity (RIN>6) and quantities were assessed using the RNA Nano 6000

Assay Kit of the Bioanalyzer 2100 system (Agilent Technologies, CA, USA). cDNA libraries were prepared from 1 µg total RNA using NEBnext Ultra TM RNA Library Prep Kit for Illumina (NEB, USA) following the manufacturer's recommendations. A total of six libraries (three each for wt and SL- leaves) were constructed and quantified using a Qubit 2.9 fluorometer (Life Technologies) and sequenced on an Illumina platform to generate paired-end reads. Raw reads of FASTQ format were processed through in-house scripts and clean reads were obtained by removing reads containing adapter, poly-N sequences and reads with low quality. A total of 35825 high-quality, clean reads were mapped using HISAT2 (79) to the reference genome of *Solanum lycopersicum* cv "Heinz 170" assembly ITAG SL3.0 (https://www.ebi.ac.uk/ena/data/view/GCA_000188115.3). Expressed genes passing quality checks, trimming and FPKM filtering are listed in Table S4. The number of mapped reads for each gene was counted using hTseq-count (80). Values of fragments per kilobase of exon per million fragments mapped (FPKM) for the assembled transcription units were calculated. After filtering and trimming, approximately 31.63 to 47.29 million clean pair-end reads were obtained from each of the six libraries. Expressed tomato genes ranged from 18261 (sample SL-_2) to 19048 (sample wt_3, Table S4), using a cut-off FPKM value > 0.3 to declare a gene as expressed. The DESeq2 R package was used to normalize expression levels and perform differential expression analysis based on the negative binomial distribution (81). Following read count normalization, the resulting P values were adjusted using the Benjamini and Hochberg's approach for controlling the False Discovery Rate (FDR). Genes with a Benjamini–Hochberg adjusted p value/FDR < 0.05 and a $\log_2$ fold change ($\log_2$FC) >+0.7;<-0.7 were assigned as DEGs. A high Pearson's correlation coefficient (r) was observed among FPKM values of biological replicates of the same genotype and condition in the sequenced set (average r = 0.92). Considering the mean of three biological replicates for each genotype, 18013 genes were found to be expressed in both lines, while 983 genes were only expressed in wt and 696 genes in SL- plants (fig. S10A). A total of 8166 protein-coding genes were found differentially expressed (DEGs) in the SL- plants with respect to wt (FDR ≤ 0.05; Dataset S3), corresponding to 23.56% of the predicted protein-coding genes. These genes were additionally filtered based on their $\log_2$ FC (thresholds -0.7 > $\log_2$FC > +0.7). After filtering, we obtained a dataset of 7140 DEGs, which display a higher proportion of down-regulated genes in the SL- plants (5412) in comparison to up-regulated genes (1728) (fig. S10B). To confirm the RNAseq results, we analyzed the expression of selected genes by qRT-PCR, focusing on flowering-related loci. Fig. S8 shows high correlation between transcript levels observed in the RNAseq dataset and in targeted qRT-PCR on independent samples.

**Functional analysis of tomato DEGs**

Enrichment analysis of each DEG gene ontology (GO) term and KEGG pathway (82) was performed with the ShinyGO v0.61 GO Enrichment Analysis tool using default parameters (http://bioinformatics.sdstate.edu/go/) (83) and comparing the frequency of query genes with the complete reference genome for *S. lycopersicum* (SL 3.0). Enrichment analyses were based on a hypergeometric distribution followed by FDR correction. Significant GO terms and KEGG functional categories (FDR < 0.05) were reported.

**Gibberellin treatments and quantification**

For the assessment of general gibberellin sensitivity, 2-week-old wt and SL- plants (n=8) were sprayed on the whole aerial part with a 10 µM solution of $GA_3$ (Sigma-Aldrich) until runoff. Control plants were sprayed with a corresponding volume of water only. The increment of the first internode length was measured every five days, starting from five days after the treatment and reported as the difference between the measured values of $GA_3$-treated and mock-treated plants of the same genotype at the same time point.

The sample preparation and analysis of gibberellins were performed as described (84) with some modifications. Briefly, tissue samples of about 5 mg dry weight (DW) from n=3 biological replicates were ground to a fine powder using 2.7-mm zirconium oxide beads (Retsch GmbH & Co. KG, Haan, Germany) and a MM 400 vibration mill at a frequency of 30 Hz for 3 min (Retsch GmbH & Co. KG, Haan, Germany) with 1 mL of ice-cold 80 % acetonitrile containing 5 % formic acid as extraction solution. The samples were then extracted overnight at 4 °C using a benchtop laboratory rotator Stuart SB3 (Bibby Scientific Ltd., Staffordshire, UK) after adding 17 internal gibberellin standards ($[^2H_2]GA_1$, $[^2H_2]GA_3$, $[^2H_2]GA_4$, $[^2H_2]GA_5$, $[^2H_2]GA_6$, $[^2H_2]GA_7$, $[^2H_2]GA_8$, $[^2H_2]GA_9$, $[^2H_2]GA_{15}$, $[^2H_2]GA_{19}$, $[^2H_2]GA_{20}$, $[^2H_2]GA_{24}$, $[^2H_2]GA_{29}$, $[^2H_2]GA_{34}$, $[^2H_2]GA_{44}$, $[^2H_2]GA_{51}$, and $[^2H_2]GA_{53}$ (OlChemIm, Czech Republic). The homogenates were centrifuged at 36,670 *g* and 4 °C for 10 min, then the corresponding supernatants were further purified using mixed-mode SPE cartridges (Waters, Milford, MA, USA) and analyzed by ultra-high performance liquid chromatography-tandem mass spectrometry (UHPLC-MS/MS; Micromass, Manchester, UK). Gibberellins were detected using multiple-reaction monitoring mode of the transition of the ion $[M–H]^{-}$ to the appropriate product ion. The Masslynx 4.2 software (Waters, Milford, MA, USA) was used to analyze the data and the standard isotope dilution method (85) was used to quantify endogenous gibberellin levels.

**Gene transcript quantification**

Total RNA from tomato leaves was extracted with the Spectrum Plant Total RNA Kit (Sigma Aldrich) and treated with DNase I (ThermoScientific) at 37°C for 30 min to remove residual genomic DNA. First-strand cDNA was synthesized from 3 µg of purified total RNA using the High-Capacity cDNA Reverse Transcription Kit (Applied Biosystems) according to the manufacturer's instructions. A modified protocol with a stem-loop primer (86) was followed for targeted miR319 and miR156 cDNA synthesis. qRT-PCR was carried out in a StepOnePlus machine (Applied Biosystems) using the SYBR method (Luna Universal One-Step RT-qPCR Kit, New England Biolabs); for loci and primers, see Table S4. Transcript concentrations were normalized on *ACTIN* (*ACT*), *ELONGATION FACTOR-1α* (*EF-1α*) or *small nuclear RNA U6* (*snU6*) transcripts as endogenous controls. Three independent biological replicates were analyzed as a minimum, and each qRT-PCR reaction was run in technical triplicates. Transcript amounts were quantified through the $2^{-\Delta\Delta Ct}$ method.

**Statistical analysis**

Significant differences among grafted plants were statistically analyzed by applying a one-way ANOVA test and Tukey's HSD post-hoc test was used for mean separation when ANOVA results were significant ($p < 0.05$). Significant differences of pairwise comparisons were assessed by Student's t test. The SPSS statistical software package (SPSS Inc., Cary, NC, v.22) was used. RNAseq results were validated via qRT-PCR as previously done (87) on genes related to flowering. In short, $log_2$FC values of *SFT* (Solyc03g063100.2), *SP5G* (Solyc05g053850.3), *SP6A* (Solyc05g055660.2), *MBP20* (Solyc02g089210.3), *FUL1* (Solyc06g069430.3), *LA* (Solyc07g062680.2), *GA2ox4* (Solyc07g061720.3), *GA20ox2* (Solyc06g035530.3), *GA3ox2* (Solyc03g119910.3) were obtained from both RNAseq and qRT-PCR analyses by contrasting SL- with wt plants. The Spearman's rank correlation method (88) was used to analyze the correlation between these two datasets. A Spearman's $\rho \geq 0.75$ was used as threshold to consider two datasets positively highly correlated.

**A**


**B**


**Fig. S1**. (**A**) Appearance of wt/wt, wt/SL- and SL-/SL- plants 30 days after grafting. (**B**) Tomato plants cv M82 at anthesis (around 5 weeks from seedling emergence). The plant on the right was treated with 5 µM $GR24^{5DS}$ 8 days after seedling emergence, while the plant on the left was mock treated at the same age.

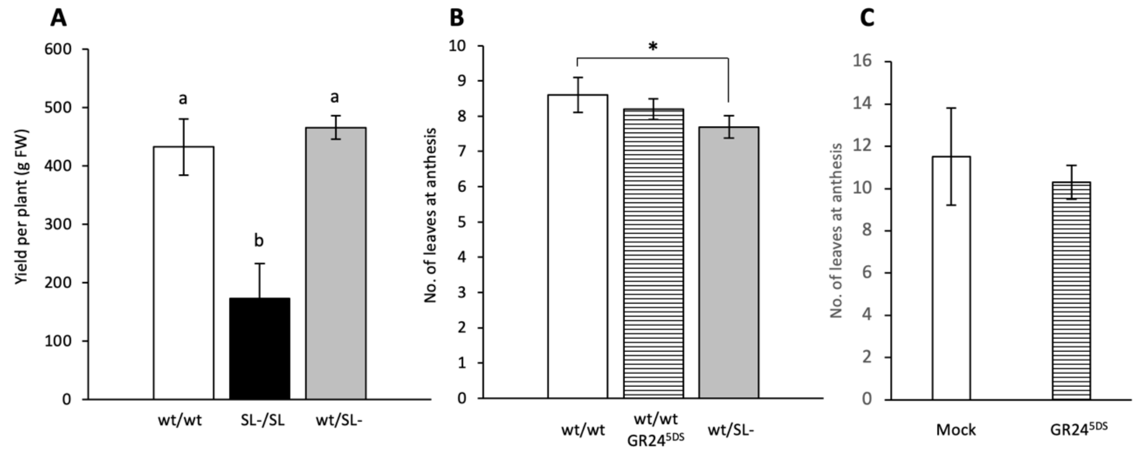


**Fig. S2.** Effects of different grafting combinations and/or treatment with 5 µM GR24$^{5DS}$ on (**A**) cumulative yield per plant in homo- or hetero-grafting of wt and strigolactone-depleted (SL-) scions and rootstocks. (**B**) Comparisons between the number of leaves at the time of anthesis in mock-treated wt/wt plants, wt/SL- plants and wt/wt plants or (**C**) non-grafted wt plants treated with 5 µM GR24$^{5DS}$ (1 and 3 weeks after grafting). Data represent the mean ± SE of n=10 biological replicates. * indicates significant differences between wt/wt plants and wt/SL- plants, as determined by Student's t test ($p < 0.05$). In panel A the letters indicate significant differences as determined by a one-way ANOVA test and Tukey's HSD post-hoc test ($p < 0.05$).

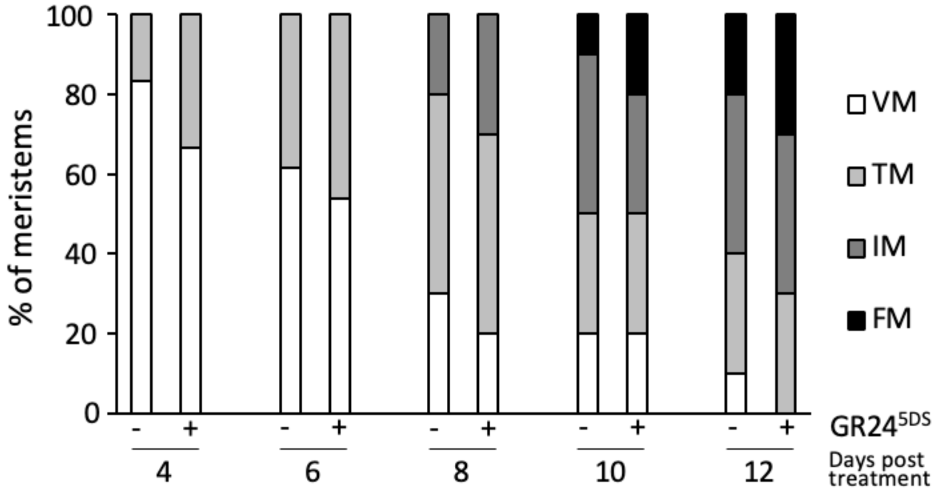


**Fig. S3.** Meristem maturation of mock- or GR24$^{5DS}$ -treated plants. For representative images of the four sequential developmental stages: vegetative meristem (VM), transition meristem (TM), inflorescence meristem (IM) and floral meristem (FM), see fig. 2A. Plants were treated with a 5 μM solution 4 days after seedling emergence, i.e. before floral transition. The meristems were evaluated under the stereomicroscope 4 to 12 days after the treatment (n=6-13).

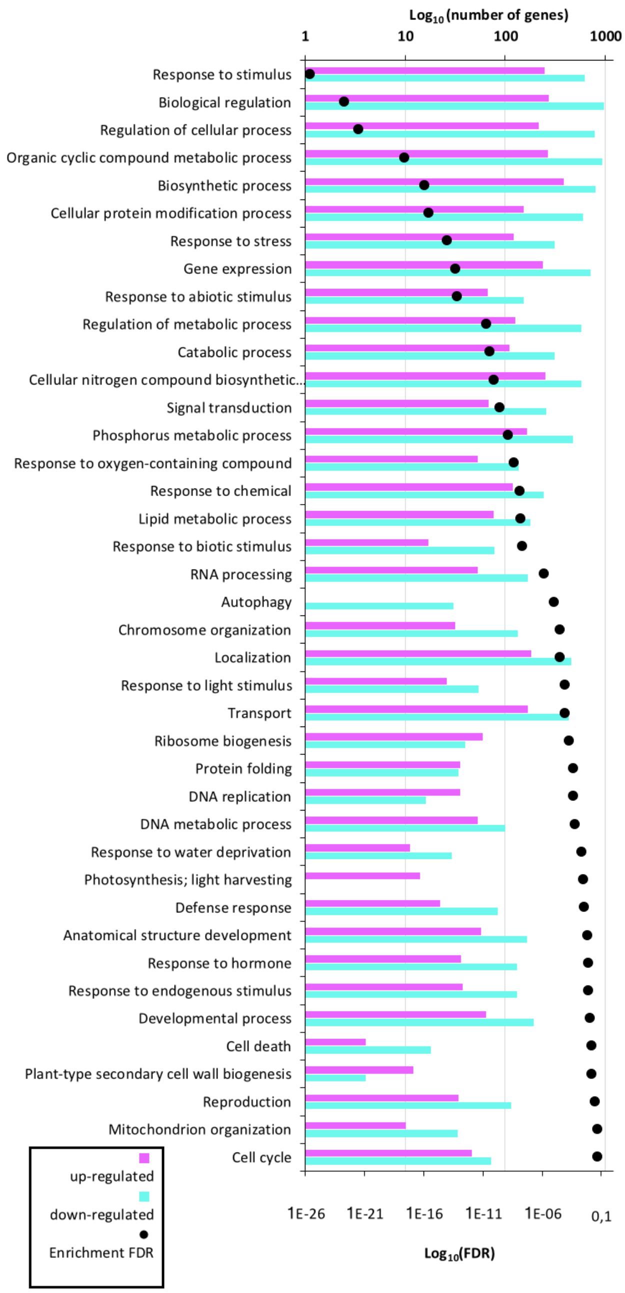


**Fig. S4**. Functional GO categories from the BP-GO enrichment of DEGs in strigolactone-depleted leaves in comparison to wt. Light blue and fuchsia bars indicate the number of up- and down-regulated DEGs, respectively. Black dots show the $Log_{10}FDR$ value of each enriched category, with FDR < 0.05 as a threshold.

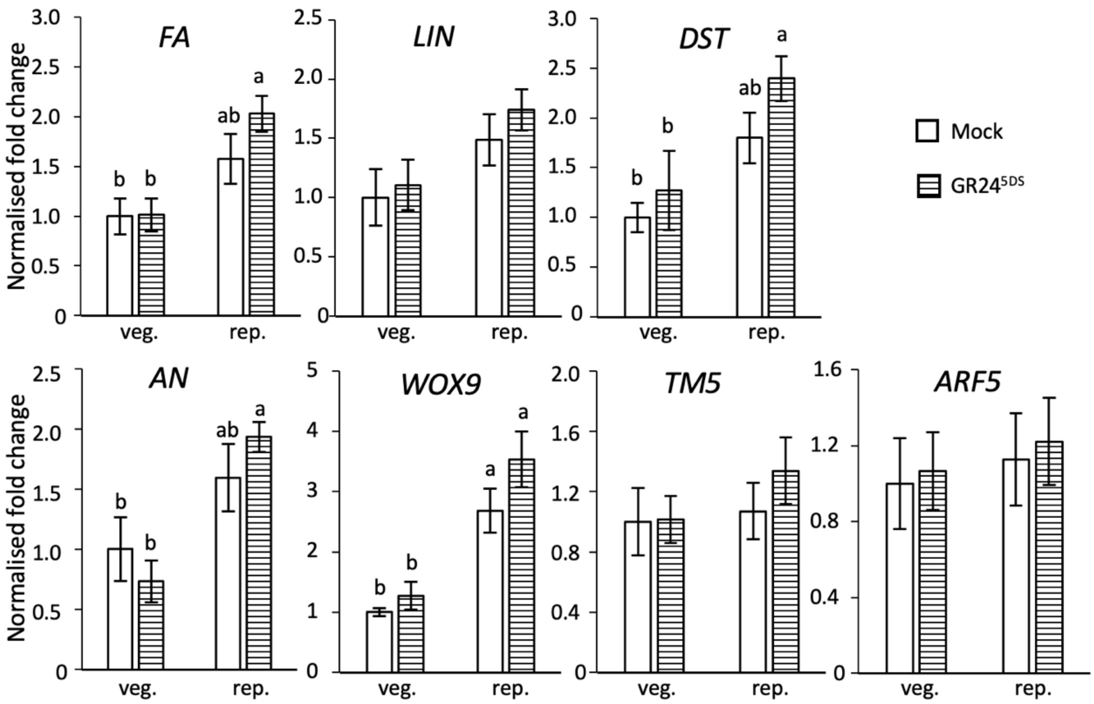


**Fig. S5.** Effects of exogenous strigolactones and age on the transcripts of marker genes for meristematic development: *FA* (*FALSIFLORA*); *LIN* (*LONG INFLORESCENCE*); *DST* (*DELAYED SYMPODIAL TERMINATION*); *AN* (*ANANTHA*); *WOX9* (*WUSCHEL-RELATED HOMEOBOX9*); *TM5* (*TOMATO MADS5*); *ARF5* (*AUXIN RESPONSE FACTOR5*). Vegetative (veg.) wt plants were treated with 5 μM $GR24^{5DS}$ 8 days after seedling emergence, and harvested one week later; another subset was treated in the reproductive (rep.) phase, 23 days after germination, and harvested 30 days after germination. Transcript abundances were normalized to endogenous *EF1α* and *ACT* and presented as fold-change value over mean values of meristems in untreated vegetative plants, which were set to 1. Data represent the mean ± SE of n=6 biological replicates (each the pool of 10 apical meristems) analyzed in technical triplicates. Different letters on top of bars indicate statistically significant differences among all samples as determined with one-way ANOVA followed by Tukey's post-hoc test; no significant differences for pairwise comparisons between treated and untreated samples of the same age could be detected by Student's t-test ($p < 0.05$).

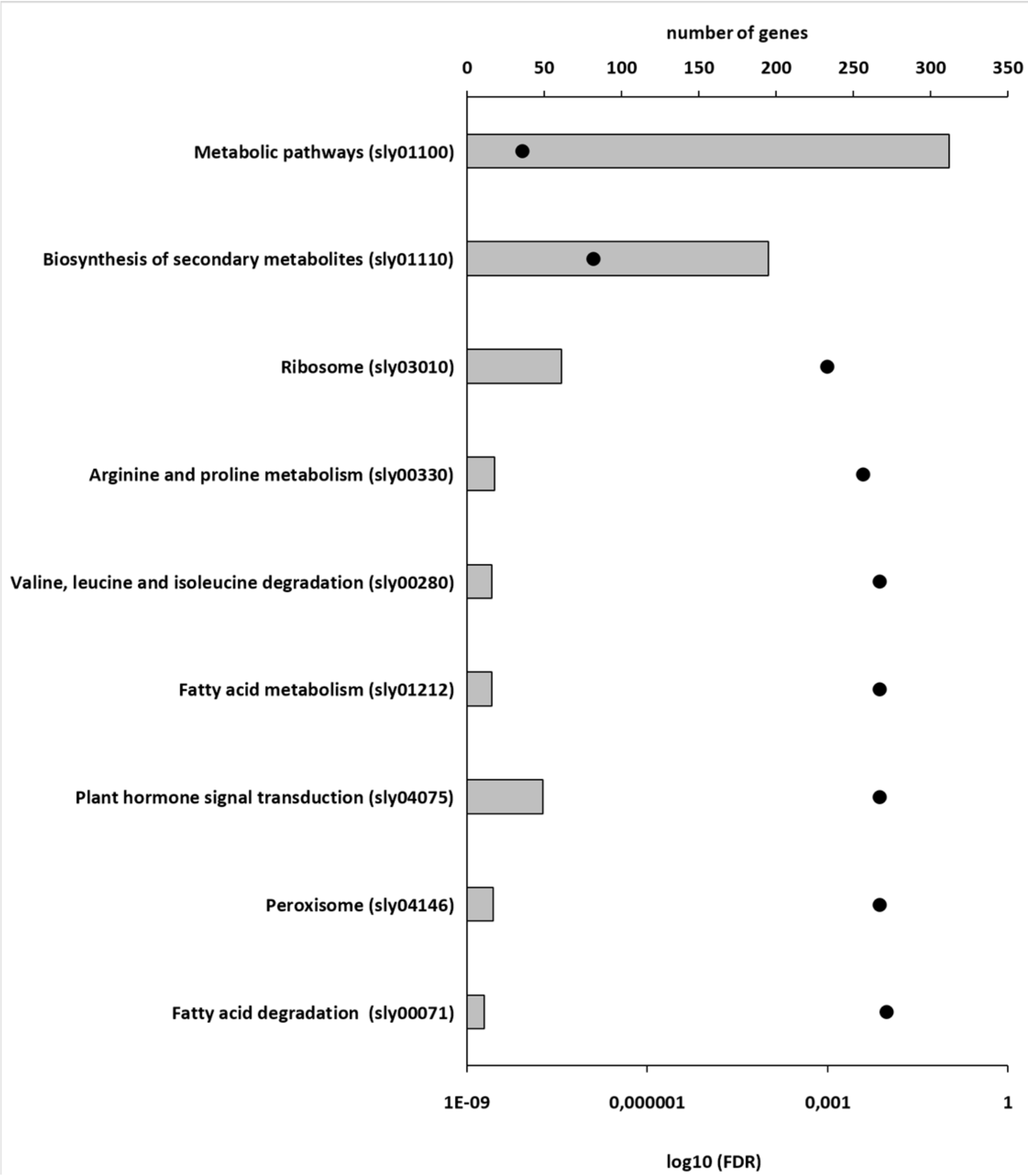


**Fig. S6.** KEGG pathways categories enriched among DEGs in leaves of strigolactone-depleted tomato plants in comparison to wt. Grey bars indicate the number of DEGs and black dots show the $Log_{10}FDR$ value for each enriched KEGG pathway category identified by the KEGG ID in brackets, with FDR < 0.05 as a threshold.

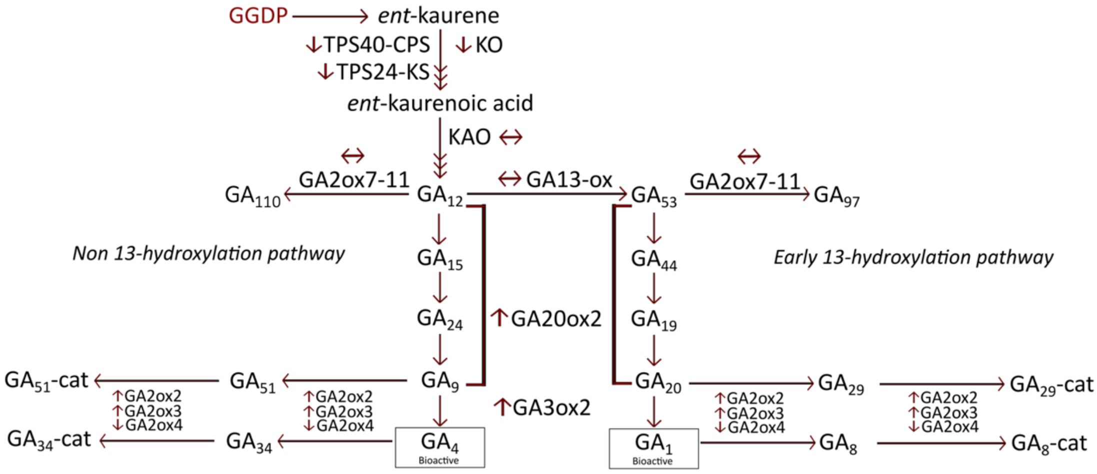


**Fig. S7.** Schematic representation of the tomato gibberellin (GA) biosynthetic pathway. GGDP, geranylgeranyl diphosphate; CPS (TPS40), *ent*-copalyl diphosphate synthase; KS (TPS24), *ent*-kaurene synthase; KO, *ent*-kaurene oxidase; KAO, *ent*-kaurenoic acid oxidase; GA13ox, GA 13-oxidase; GA20ox, GA 20-oxidase; GA3ox, GA 3-oxidase; GA2ox, GA 2-oxidase; GA-cat, GA-catabolite. Arrows by gene acronyms indicate whether each gene is up- or down-regulated, or remains stable in strigolactone-depleted plants compared to the wt.

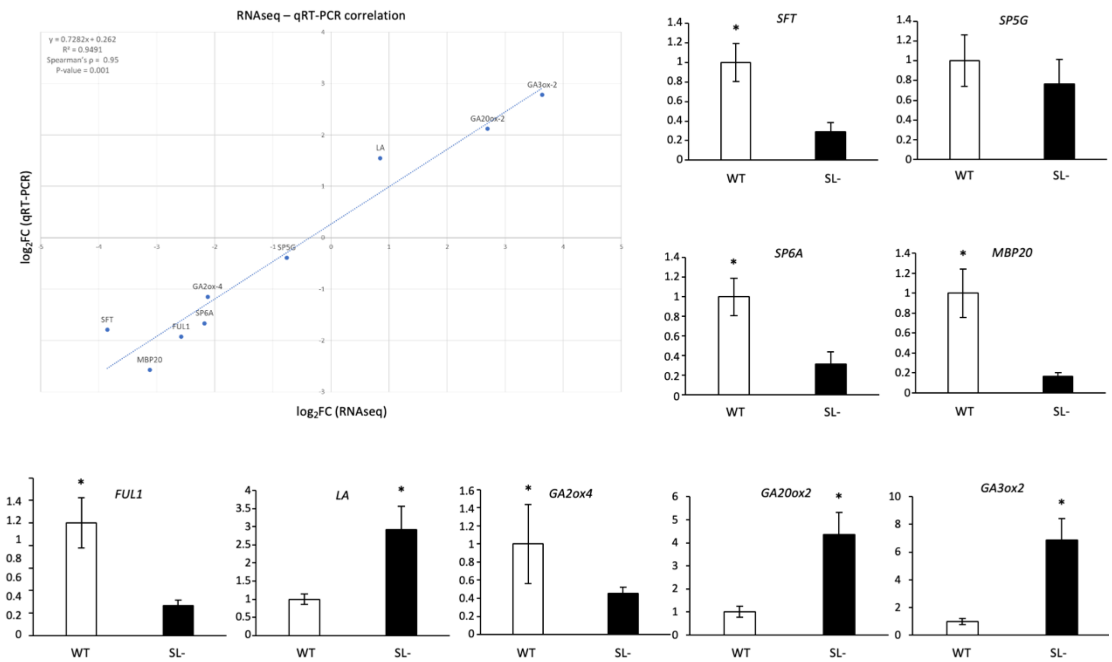


**Fig. S8.** RNAseq validation through qRT-PCR analysis. **Upper left:** correlation between RNAseq (x-axis) and qRT-PCR (y-axis) $\log_2$FC values of transcripts obtained by comparing strigolactone-depleted (SL-) and wt plants. Correlation was calculated through the Spearman's rank correlation method (Spearman's ρ and p-value, $R^2$ and best-fit line equation are shown). **All other panels:** validation of the RNAseq analysis by qRT-PCR. Transcript quantification of *SFT* (Solyc03g063100.2); *SP5G* (Solyc05g053850.3); *SP6A* (Solyc05g055660.2); *MBP20* (Solyc02g089210.3); *FUL1* (Solyc06g069430.3); *LA* (Solyc07g062680.2); *GA2ox4* (Solyc07g061720.3); *GA20ox2* (Solyc06g035530.3); *GA3ox2* (Solyc03g119910.3). Transcript abundances were normalized to endogenous *EF1α* and *ACT* and presented as fold-change values over mean values of wt plants, which were set to 1. Data represent the mean ± SE of n=3 biological replicates. * indicates significant differences as determined by Student's t test ($p < 0.05$).

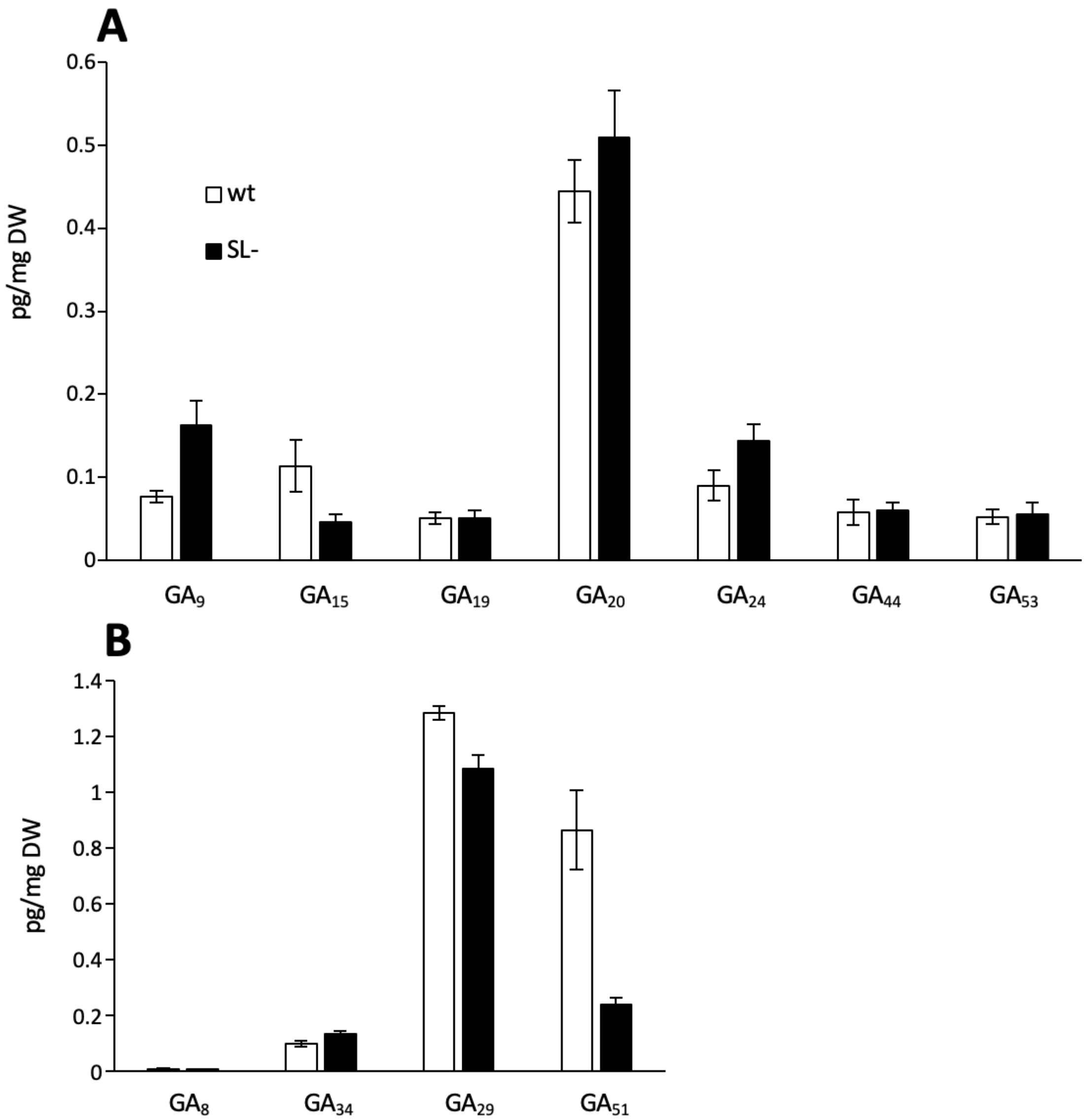


**Fig. S9.** Effect of strigolactone deprivation on gibberellin metabolism. (**A**) Concentration of the biosynthetic precursors of bioactive gibberellins and (**B**) of their deactivation products in wt and strigolactone-depleted (SL-) plants. Data represent the mean ± SE of n=3 biological replicates analyzed in technical quadruplicates. See fig. S7 for metabolite positioning in the gibberellin pathway.

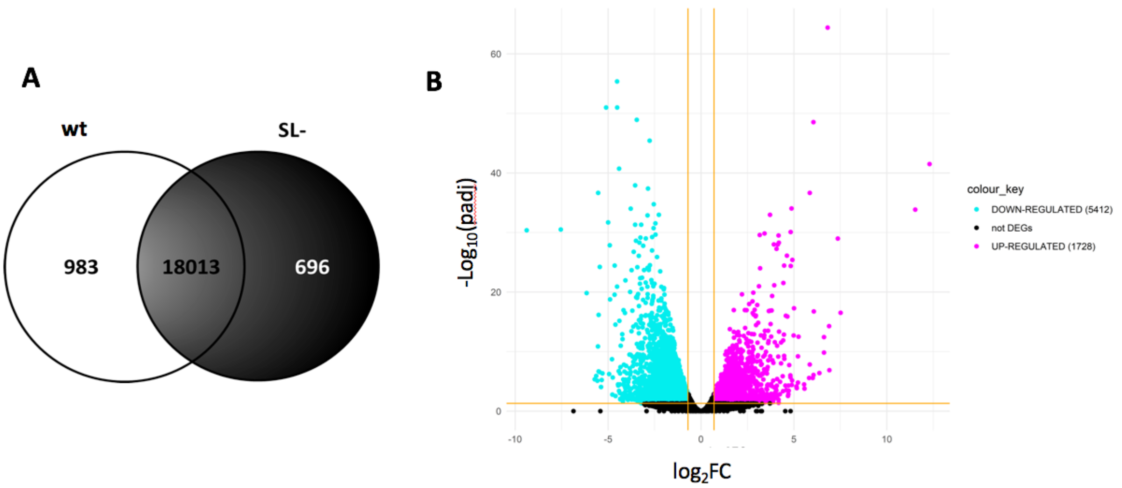


**Fig. S10.** Comparison of expressed genes between wt and strigolactone-depleted (SL-) tomato lines. (**A**) Venn diagram displaying the number of genes identified in either or both genotypes; (**B**) volcano plot of the number and distribution of up- and down-regulated DEGs (FDR < 0.05, $log_2FC$ >+0.7 and <-0.7 respectively), showing statistical significance (padjust) versus magnitude of change (fold change, FC).

**Table S1.** Selection of tomato DEGs between wt and strigolactone-depleted leaves related to flowering and/or included in the GO category Reproduction (GO: 0000003). A comprehensive list of all DEGs related to this category can be found in Dataset S2.

| **Gene ID** | **log$_2$FC** | **ITAG3.0 annotation** | ***S. lycopersicum* gene acronym** | ***A. thaliana* orthologue** | ***A. thaliana* acronym** |
|---|---:|---|---|---|---|
| Solyc03g119910.3 | 3.64 | *Le3OH-23b-hydroxylase* | *GA3ox2* | AT1G15550 | *GA3OX1* |
| Solyc04g054150.1 | 2.84 | *Nuclear transcription factor Y protein* | *NF-YB3* | AT4G14540 | *NF-YB3* |
| Solyc06g035530.3 | 2.70 | *Gibberellin 20-oxidase-2* | *GA20ox2* | AT5G51810 | *GA20OX2* |
| Solyc08g005610.3 | 2.29 | *Abscisic acid 8'-hydroxylase* | *CYP707A2* | AT5G45340 | *CYP707A3* |
| Solyc04g071990.3 | 2.15 | *GIGANTEA* | *GI* | AT1G22770 | *GI* |
| Solyc06g069230.3 | 1.98 | *DNA mismatch repair protein* | *MSH2* | AT3G18524 | *MSH2* |
| Solyc03g093610.1 | 1.67 | *Ethylene response factor A.2* | *ERFA2* | AT5G47220 | *ERF2* |
| Solyc03g115050.3 | 1.63 | *Replication A 70 kDa DNA-binding subunit* | *RPA1B* | AT5G08020 | *RPA1B* |
| Solyc11g072600.2 | 1.14 | *APETALA 2d* | *AP2d* | AT2G28550 | *TOE1* |
| Solyc07g006630.3 | 0.97 | *CONSTANS-like protein* | *COL* | AT5G15850 | *CO* |
| Solyc07g062680.2 | 0.85 | *Lanceolate* | *LA* | AT3G15030 | *TCP4* |
| Solyc02g084630.3 | -0.72 | *TDR6 transcription factor* | *TM6/TDR6* | AT5G23260 | *AGL32/TT16* |
| Solyc05g053850.3 | -0.76 | *SELF PRUNING 5G* | *SP5G* | AT1G65480 | *FT* |
| Solyc11g010570.2 | -0.78 | *Jointless* | *J* | AT2G22540 | *AGL22/SVP* |
| Solyc12g056460.2 | -1.07 | *MADS box transcription factor* | *MBP14* | AT2G45660 | *AGL20* |
| Solyc12g096500.2 | -1.08 | *CONSTANS-like protein* | *COL4a* | AT5G24930 | *COL4* |
| Solyc03g121010.3 | -1.21 | *RNA polymerase II-associated factor 1 like* | *ELF7* | AT1G79730 | *ELF7* |
| Solyc01g079870.3 | -1.21 | *CONSTANS interacting protein 2b* | *NF-YC9* | AT1G08970 | *NF-YC9* |
| Solyc10g009080.3 | -1.36 | *Squamosa promoter binding protein 3* | *SBP3* | AT2G33810 | *SPL3* |
| Solyc11g011980.2 | -1.37 | *Transducin/WD40 repeat-like superfamily protein* | *COP1* | AT2G32950 | *COP1* |
| Solyc02g089540.3 | -1.40 | *CONSTANS 1* | *CO1* | At5G15841 | *CO* |
| Solyc03g006830.3 | -1.46 | *MADS-box transcription factor* | *MBP18/FYFL* | AT5G62165 | *AGL42* |
| Solyc01g098390.3 | -1.52 | *Gibberellin receptor* | *GID1a* | AT3G05120 | *GID1A* |
| Solyc03g117670.3 | -1.55 | *Snf1-related kinase interacting protein* | *SKI2* | AT1G80940 | - |
| Solyc09g074270.3 | -1.57 | *Gid1-like gibberellin receptor* | *GID1b1* | AT3G63010 | *GID1B* |
| Solyc01g008490.3 | -1.61 | *Nuclear transcription factor Y subunit* | *NF-YA1* | AT5G12840 | *NF-YA1* |

| | | | | | |
|---|---|---|---|---|---|
| Solyc10g005080.3 | -1.64 | *Late elongated hypocotyl and circadian clock associated-1-like protein 1* | *LHY* | AT1G01060 | *LHY* |
| Solyc08g065870.3 | -1.69 | *EARLY FLOWERING 3* | *ELF3* | AT2G25930 | *ELF3* |
| Solyc08g006570.3 | -1.70 | *ANAPHASE-PROMOTING COMPLEX 13 Bonsai protein* | *Solyc08g006570* | AT1G73177 | *APC13/BNS* |
| Solyc11g010120.2 | -1.72 | *Peroxidase* | *PER17* | AT2G22420 | *PRX17* |
| Solyc02g084740.3 | -1.87 | *Cytochrome P–50 - 3-epi-6-deoxocathasterone 23-monooxygenase* | *CYP90C2/DUMPY* | AT4G36380 | *ROT3* |
| Solyc01g087240.3 | -1.96 | *Nuclear transcription factor Y subunit A-9* | *NF-YA9* | AT3G20910 | *NF-YA9* |
| Solyc07g061720.3 | -2.12 | *Gibberellin 2-oxidase 4* | *GA2ox4* | AT1G78440 | *GA2OX1* |
| Solyc08g062210.3 | -2.13 | *Nuclear transcription factor Y subunit* | *NF-YA8* | AT1G17590 | *NF-YA8* |
| Solyc08g080100.3 | -2.17 | *MADS-box transcription factor* | *MBP13* | AT4G22950 | *AGL19* |
| Solyc05g055660.2 | -2.18 | *Flowering locus T protein* | *SP6A* | AT1G65480 | *FT* |
| Solyc07g049530.3 | -2.22 | *1-Aminocyclopropane-1-carboxylate oxidase 1* | *ACO1* | AT2G19590 | *ACO1* |
| Solyc07g062840.3 | -2.25 | *Goblet* | *GOBLET* | AT5G53950 | *CUC2* |
| Solyc03g115770.2 | -2.40 | *Timing of cab expression 1/pseudo-response regulator 1* | *TOC1* | AT5G61380 | *TOC1* |
| Solyc09g090890.2 | -2.41 | *DNA mismatch repair protein* | *MSH1* | AT3G24320 | *MSH1* |
| Solyc06g069710.3 | -2.42 | *NAC domain protein* | *NAM3* | AT5G61430 | *NAC100* |
| Solyc03g115850.3 | -2.52 | *NAC domain-containing protein* | *NAM2* | AT5G61430 | *NAC100* |
| Solyc06g069430.3 | -2.58 | *FRUITFULL-like MADS-box 1* | *FUL1* | AT3G30260 | *AGL79* |
| Solyc01g006930.3 | -2.88 | *Nuclear transcription factor Y subunit A-10, putative* | *NF-YA10* | AT5G06510 | *NF-YA10* |
| Solyc12g087830.2 | -2.98 | *MADS-box transcription factor* | *MBP15* | AT1G47760 | *AGL102* |
| Solyc11g020290.2 | -3.07 | *WD-40 repeat-containing protein MSI1* | *WDR238* | AT5G58230 | *MSI1* |
| Solyc02g089210.3 | -3.12 | *MADS box transcription factor* | *MBP20* | AT1G69120 | *AP1* |
| Solyc02g089520.2 | -3.46 | *CONSTANS protein* | *CO3* | At5G15840 | *CO* |

| | | | | | |
|---|---|---|---|---|---|
| Solyc12g009050.2 | -3.46 | *Nuclear transcription factor Y subunit* | *NF-YA3* | AT1G72830 | *NF-YA3* |
| Solyc03g063100.2 | -3.85 | *Single flower truss* | *SP3D; SFT* | AT1G65480 | *FT* |
| Solyc12g042967.1 | -3.87 | *Agamous-like MADS-box protein AGL80* | *MADS56* | AT5G48670 | *AGL80* |
| Solyc06g051680.1 | -4.13 | *Protein EARLY FLOWERING 4* | *ELF4* | AT2G40080 | *ELF4* |
| Solyc04g005610.3 | -4.51 | *NAC domain protein NAC2* | *NAP2* | AT1G69490 | *NAC029* |
| Solyc03g114830.3 | -4.75 | *FRUITFULL-like MADS-box 2* | *MBP7/FUL/FUL2* | AT5G60910 | *AGL8* |

**Table S2.** Tomato DEGs involved in auxin biosynthesis and metabolism ([GO:0009851] and [GO:0009850]), transport and export ([GO:0009926] and [GO:0010315]), and responses ([GO:0009734] and [GO:0009733]) as retrieved after the differential expression analysis.

| Gene ID | $log_2FC$ | ITAG 3.0 annotation | *S. lycopersicum* gene acronym | *A. thaliana* orthologue | *A. thaliana* gene acronym |
|---|---|---|---|---|---|
| **auxin biosynthetic process [GO:0009851], auxin metabolic process [GO:0009850]** | | | | | |
| Solyc09g064160.3 | 3.815015 | *Flavin-containing monooxygenase* | *Solyc09g064160* | AT4G28720 | *YUC8* |
| Solyc05g006220.3 | -1.77763 | *IAA-amino acid hydrolase* | *Solyc05g006220* | AT1G51760 | *IAR3* |
| Solyc05g006220.4 | 0.844649 | *IAA-amino acid hydrolase* | *Solyc05g006220* | AT1G51760 | *IAR3* |
| Solyc05g006220.5 | 0.988377 | *IAA-amino acid hydrolase* | *Solyc05g006220* | AT1G51760 | *IAR3* |
| **auxin polar transport [GO:0009926], auxin export across the plasma membrane [GO:0010315]** | | | | | |
| Solyc02g089263.1 | -0.93593 | *Auxin transport protein BIG* | *Solyc02g089263* | AT3G02260 | *TIR3* |
| Solyc05g026140.3 | -0.70524 | *Uncharacterized protein* | *Solyc05g026140* | AT2G31190 | *RUS2* |
| Solyc01g099120.3 | 0.65156 | *Auxin response 4* | *AXR4* | AT1G54990 | *AXR4* |
| Solyc03g118740.3 | 0.89916 | *Auxin efflux facilitator* | *PIN1* | AT1G73590 | *PIN1* |
| Solyc10g078370.2 | -0.90325 | *Auxin efflux facilitator* | *PIN9* | AT1G73590 | *PIN1* |
| **auxin-activated signaling pathway [GO:0009734], response to auxin [GO:0009733]** | | | | | |
| Solyc03g114480.3 | -2.84071 | *Tetraspanin-8* | *Solyc03g114480* | AT4G28050 | *TET7* |
| Solyc04g076850.3 | -1.35286 | *Entire* | *E* | AT5G65670 | *IAA9* |
| Solyc11g072480.2 | 2.37454 | *Tetraspanin-3* | *Solyc11g072480* | AT3G45600 | *TET3* |
| Solyc02g082450.3 | -1.34272 | *Auxin efflux facilitator* | *Solyc02g082450* | AT2G17500 | *PIN-likes5* |
| Solyc02g079190.3 | -1.09298 | *Auxin F-box protein 5* | *Solyc02g079190* | AT3G62980 | *TIR1* |
| Solyc03g059390.3 | -1.42873 | *Tetraspanin-2* | *TET2* | AT2G19580 | *TET2* |
| Solyc01g096070.3 | -1.18782 | *Auxin response factor 18* | *ARF18* | AT4G23980 | *ARF9* |
| Solyc04g049080.3 | -1.11164 | *Tetraspanin-6* | *Solyc04g049080* | AT4G23410 | *TET5* |
| Solyc02g077560.3 | -0.85503 | *Auxin response factor 3* | *Solyc04g049080* | AT2G33860 | *ARF3* |
| Solyc12g042075.1 | -0.77682 | *Auxin-response factor* | *Solyc12g042075* | AT5G62000 | *ARF2* |
| Solyc03g120380.3 | 1.30301 | *Auxin-regulated IAA19* | *IAA19* | AT3G15540 | *IAA19* |
| Solyc04g082830.3 | -1.85963 | *Auxin efflux carrier family protein* | *Solyc04g082830* | AT1G20925 | *PIN-likes1* |
| Solyc02g037550.3 | -1.54635 | *Auxin efflux carrier family protein* | *Solyc02g037550* | AT1G76520 | *PIN-likes3* |
| Solyc03g031990.3 | -0.89102 | *Auxin efflux carrier family protein* | *Solyc03g031990* | AT1G76520 | *PIN-likes3* |
| Solyc02g091240.1 | -0.76972 | *Auxin efflux carrier family protein* | *Solyc02g091240* | AT1G71090 | *PIN-likes2* |
| Solyc11g069500.2 | -0.71450 | *Auxin response factor 10A* | *ARF10A* | AT2G28350 | *ARF10* |
| Solyc06g075360.3 | 1.14777 | *Tetraspanin-3-like* | *Solyc06g075360* | AT3G45600 | *TET3* |
| Solyc12g007230.2 | -0.77621 | *Auxin-regulated IAA8* | *IAA8* | AT4G29080 | *IAA27* |
| Solyc08g082630.3 | -1.12841 | *Auxin response factor 9A* | *ARF9A* | AT4G23980 | *ARF9* |
| Solyc07g025510.3 | -0.74116 | *Senescence-associated protein* | *Solyc07g025510* | AT2G19580 | *TET2* |

| | | | | | |
|---|---|---|---|---|---|
| Solyc06g053840.3 | -0,74270 | *Auxin-regulated IAA4* | *IAA4* | AT5G43700 | *IAA4* |
| Solyc08g080730.3 | -0.94883 | *Tetraspanin-10* | *Solyc08g080730* | AT1G56700 | *TET10* |
| Solyc03g116100.3 | -2.08677 | *R2R3MYB transcription factor 31* | *MYB31* | AT5g62470 | *MYB5* |
| Solyc07g014620.1 | -2.55421 | *Small auxin up-regulated RNA63* | *SAUR63* | AT5G20810 | *SAUR70* |
| Solyc06g053260.1 | -1.29932 | *Small auxin up-regulated RNA 58* | *SAUR58* | AT4G00880 | *SAUR31* |
| Solyc02g067340.3 | 1.44044 | *R2R3MYB transcription factor 96* | *THM6* | AT3G47600 | *MYB94* |
| Solyc01g110680.3 | -1.33216 | *Small auxin up-regulated RNA12* | *SAUR12* | AT2G21210 | *SAUR6* |
| Solyc02g087960.3 | 2.57066 | *R2R3MYB transcription factor 94* | *MYB94* | AT3G47600 | *MYB94* |
| Solyc11g011660.2 | 1.46882 | *Auxin-induced SAUR* | *Solyc11g011660* | AT1G29500 | *SAUR66* |
| Solyc10g083320.2 | 3.74462 | *Small auxin up-regulated RNA82* | *SAUR82* | AT2G36210 | *SAUR45* |
| Solyc01g111000.3 | -1.42006 | *Auxin-induced SAUR-like* | *Solyc01g111000* | AT4G38840 | *SAUR14* |
| Solyc01g096340.3 | -0.72682 | *Small auxin up-regulated RNA2* | *SAUR2* | AT3G61900 | *SAUR33* |
| Solyc04g052970.2 | 1.98848 | *Auxin-induced SAUR-like* | *Solyc04g052970* | AT5G18030 | *SAUR21* |
| Solyc01g110560.3 | -1.02335 | *Small auxin up-regulated RNA3* | *SAUR3* | AT4G34750 | *SAUR49* |
| Solyc01g110940.3 | 1.27774 | *Auxin-induced SAUR-like* | *Solyc01g110940* | AT4G38840 | *SAUR14* |
| Solyc01g110590.3 | 1.23355 | *Small auxin up-regulated RNA6* | *SAUR6* | AT4G34760 | *SAUR50* |
| Solyc04g078900.3 | 0.95678 | *Abscisic acid 8'-hydroxylase CYP707A1* | *CYP707A1* | AT3G19270 | *CYP707A4* |
| Solyc04g053000.1 | 1.33901 | *Auxin-induced SAUR-like* | *Solyc04g053000* | AT5G18030 | *SAUR21* |
| Solyc06g053290.1 | -0.73484 | *Small auxin up-regulated RNA59* | *SAUR59* | AT2G46690 | *SAUR32* |

**Table S3.** Tomato DEGs involved in gibberellin signalling (included in the KEGG ID: sly04075) and biosynthesis (included in the KEGG ID: sly01110) as retrieved from KEGG maps after the enrichment analysis.

| **Gene ID** | **$log_2FC$** | **ITAG 3.0 annotation** | ***S. lycopersicum* gene acronym** | ***A. thaliana* orthologue** | ***A. thaliana* gene acronym** |
|---|---|---|---|---|---|
| **GA signalling** | | | | | |
| Solyc04g078390.2 | -0.72 | *F-box family protein* | *SLY1* | AT4G24210 | *SLY1 (GID2)* |
| Solyc01g098390.3 | -1.52 | *Gibberellin receptor GID1A* | *GID1a* | AT5G27320 | *GID1C* |
| Solyc09g074270.3 | -1.57 | *Gid1-like gibberellin receptor* | *GID1b1* | AT3G63010 | *GID1B* |
| Solyc01g102300.3 | -2.81 | *bHLH transcription factor 006* | *PIF3* | AT1G09530 | *PIF3* |
| **GA metabolism** | | | | | |
| Solyc03g119910.3 | 3.64 | *Le3OH-23b-hydroxylase* | *GA3ox-2* | AT1G15550 | *GA3OX1* |
| Solyc06g035530.3 | 2.70 | *Gibberellin 20-oxidase-2* | *GA20ox-2* | AT4G25420 | *GA20OX1* |
| Solyc07g056670.3 | 2.60 | *Gibberellin 2-oxidase 2* | *GA2ox-2* | AT1G78440 | *GA2OX1* |
| Solyc01g079200.3 | 2.29 | *Gibberellin 2-oxidase 3* | *GA2ox-3* | AT1G02400 | *GA2OX6* |
| Solyc07g066675.1 | -1.30 | Ent-*kaurene synthase* | *TPS24* (*KS*) | AT1G79460 | *GA2* |
| Solyc07g066670.3 | -1.62 | Ent-*kaurene synthase* | *TPS24* (*KS*) | AT1G79460 | *GA2* |
| Solyc07g061720.3 | -2.12 | *Gibberellin 2-oxidase-4* | *GA2ox-4* | AT1G78440 | *GA2OX1* |
| Solyc04g083160.2 | -2.44 | *Cytochrome P450* | *KO* | AT5G25900 | *KO* |
| Solyc06g084240.2 | -4.09 | *Copalyl diphosphate synthase* | *TPS40* (*CPS*) | AT4G02780 | *GA1* |

**Table S4.** Expressed genes passing quality checks, trimming and FPKM filtering in 3 independent replicates of wild-type *Solanum lycopersicum* M82 (wt) or *CCD7*-silenced leaves in the same background (SL-). SL 3.0: *Solanum lycopersicum* (tomato) genome assembly SL3.0 from the Solanaceae Genomics Project.

| **Sample** | **No. of clean reads x $10^6$** | **Aligned reads on SL 3.0 (%)** | **No. of expressed transcripts** |
|---|---|---|---|
| wt_1 | 47.29 | 85.45 | 18791 |
| wt_2 | 42.92 | 84.64 | 18615 |
| wt_3 | 31.63 | 85.40 | 19048 |
| SL-_1 | 32.06 | 85.25 | 18702 |
| SL-_2 | 36.99 | 86.75 | 18261 |
| SL-_3 | 39.09 | 86.96 | 18626 |

**Table S5.** List of primers used in this work, with target gene names.

| **primer/ target** | **sequence** | **reference** |
|---|---|---|
| *ACT* | 5'-TCCCAGGTATTGCTGATAGAA-3'<br>5'-TGAGGGAAGCCAAGATAGAG -3' | (89) |
| *AN* | 5'-CCATAATTCCCCTGCCTCCA-3'<br>5'-TCCCCTGTACATGCACCATT-3' | This work |
| *AP1/MC* | 5'-CGAGAAAGAACCAACTCATGC-3'<br>5'-TAGTTTGCTGGTGCCATTCA-3' | (90) |
| *ARF5* | 5'-ATTAGTTCTGAGTTGTGGC-3'<br>5'-GGTATCTGTGAAGTTGCTG-3 | (91) |
| *DOF9* | 5'-ATGGTGCTGGAGCGAGTATG-3'<br>5'-GCGTAGAAATAGCAAGATCTGGGA-3' | This work |
| *DST* | 5'-TTTGCCTGTGGAGAGGAGAGGAAA-3'<br>5'-ACTCAACGCGCAGAACGTAACGAT-3' | This work |
| *EF-1α* | 5'-CTCCATTGGGTCG TTTTGCT-3'<br>5'-GGTCACCTTGGC ACCAGTTG-3' | (92) |
| *FA* | 5'-AGGGGAAGAGGATGAGGAAA-3'<br>5'-GATGCTCCCTTTGTCTCTCG-3' | (90) |
| *FUL1* | 5'-GTTTTGCCACAACAACTGGACTC-3'<br>5'-CTTGCTGCTGTGAAGAACTACC-3' | (93) |
| *GA20ox2* | 5'-TTTCCATATTCTACCCTACAAG -3'<br>5'-TCATCGCATTACAATACTCTT -3' | (94) |
| *GA2ox4* | 5'-CCAACAACACTTCCGGTCTT-3'<br>5'-CATTCGTCATCACCTGTAATGAG-3' | (19) |
| *GA3ox2* | 5'-GATCATAAATTTGTCATGGATAC -3'<br>5'-TGTTTCCATATGGTTAAGTAATCG -3' | (95) |
| *LA* | 5'-TGCAGCAGCTATTCGGTCAA-3'<br>5'-ACCCAGAGAATCCGCCTACT-3' | (10) |
| *LIN* | 5'-AGTGCCAAACAGGTACAATGTG-3'<br>5'-CCATTCAAAGCATCCATCCTGG-3' | This work |
| *MBP20* | 5'-CACATTCTCACCACCAACTTCCTAA-3'<br>5'-AGTGATGAGCCTGACCGGAT-3' | (40) |
| *SBP3* | 5'-CAAGTTGAACGGGCACCTAC-3'<br>5'-TGGCAAATGACAGAAGAGAGAG-3' | (90) |
| *SBP15* | 5'-GGTTCAGCTACCAGGACCAG-3'<br>5'-TGTGAACTTGGCTGTTGACC-3' | (90) |
| *SFT* | 5'-GTCACCGATATTCCAGCTACC-3'<br>5'-CATACACTGTTTGCCGACCTA-3' | This work |
| *snRU6* | 5'-GGGAACGATACAGAGAAGATTAGC-3'<br>5'-ACCATTTCTCGATTTGTGCGT-3' | (22) |
| *SP5G* | 5'-CTAGCAACCCAAACCTGAGG-3'<br>5'-ATTGCCAAAGGTTGCTCCTG-3' | This work |

| | | |
|---|---|---|
| *SP6A* | 5’-TGGTCGTGTGATAGGTGAAGT-3’<br>5’-CTGTGACCAGCCAGTGTAGA-3’ | This work |
| *TR5* | 5’-GCAGCGATCACAGAGGAATC-3’<br>5-TGGCTTCCTTCCATCAACCT-3’ | This work |
| *UF* | 5’-CCCCGGTGGTTCTAAAATGG-3’<br>5’-TCAACTTGTTGAAAGGCATCGT-3’ | This work |
| *WOX9* | 5’-TGCAGTCACAGCTCATGAGT-3’<br>5’-TCCCAACCTCAAAAGCAACG-3’ | This work |
| Stem-loop miR156 | 5’-GTCGTATCCAGTGCAGGGTCCGAGGTATTCGCACTGGATACGACGTGCTC-3’ | (96) |
| Mature miR156 | 5'-GTCGTATCCAGTGCAGGGT-3’<br>5'-TTGACAGAAGATAGAGAGCACG-3’ | (22) |
| Stem-loop miR319 | 5’-GTCGTATCCAGTGCAGGGTCCGAGGTATTCGCACTGGATACGAGGGAGC-3’ | (97) |
| Mature miR319 | 5’-GCGGCGTTGGACTGAAGGGT-3’<br>5’-GTGCAGGGTCCGAGG-3’ | (97) |

**Dataset S1** (separate file). Gene ontology categories for Biological Processes (BP-GO) enriched in strigolactone-depleted (SL-) tomato leaves in comparison to wt (FDR<0.05; $log_2$FC >+0.7;<-0.7), obtained using the ShinyGO v0.61 Gene Ontology Enrichment Analysis tool.

**Dataset S2** (separate file). List of DEGs included in the GO category Reproduction (GO: 0000003).

**Dataset S3** (separate file). List of differentially expressed genes (DEGs) in the strigolactone-depleted (SL-) plants with respect to wt (padjust ≤ 0.05).

## SI References


54. R. Wang *et al.*, Re-evaluation of transcription factor function in tomato fruit development and ripening with CRISPR/Cas9-mutagenesis. *Sci. Rep.* **9**, 1696 (2019).
55. E. Gimenez *et al.*, *TOMATO AGAMOUS1* and *ARLEQUIN/TOMATO AGAMOUS-LIKE1* MADS-box genes have redundant and divergent functions required for tomato reproductive development. *Plant Mol. Biol.* **91**, 513-531 (2016).
56. X. Ma *et al.*, The NAC transcription factor SlNAP2 regulates leaf senescence and fruit yield in tomato. *Plant Physiol.* **177**, 1286-1302 (2018).
57. Y. Berger *et al.*, The NAC-domain transcription factor GOBLET specifies leaflet boundaries in compound tomato leaves. *Development* **136**, 823-832 (2009).
58. A. Hendelman, R. Stav, H. Zemach, T. Arazi, The tomato NAC transcription factor SlNAM2 is involved in flower-boundary morphogenesis. *J. Exp. Bot.* **64**, 5497-5507 (2013).
59. C. Bendix, C. M. Marshall, F. G. Harmon, Circadian clock genes universally control key agricultural traits. *Mol. Plant* **8**, 1135-1152 (2015).
60. P. Facella *et al.*, Diurnal and circadian rhythms in the tomato transcriptome and their modulation by cryptochrome photoreceptors. *PLoS One* **3**, e2798 (2008).
61. Y. Tanigaki *et al.*, Transcriptome analysis of plant hormone-related tomato (*Solanum lycopersicum*) genes in a sunlight-type plant factory. *PLoS One* **10**, e0143412 (2015).
62. R. Schaffer *et al.*, The late elongated hypocotyl mutation of Arabidopsis disrupts circadian rhythms and the photoperiodic control of flowering. *Cell* **93**, 1219-1229 (1998).
63. J. L. Pruneda-Paz, G. Breton, A. Para, S. A. Kay, A functional genomics approach reveals CHE as a component of the Arabidopsis circadian clock. *Science* **323**, 1481-1485 (2009).
64. X. W. Deng, T. Caspar, P. H. Quail, *COP1*: a regulatory locus involved in light-controlled development and gene expression in Arabidopsis. *Genes Dev.* **5**, 1172-1182 (1991).
65. S. Jang *et al.*, Arabidopsis COP1 shapes the temporal pattern of CO accumulation conferring a photoperiodic flowering response. *EMBO J.* **27**, 1277-1288 (2008).
66. M. R. Doyle *et al.*, The *ELF4* gene controls circadian rhythms and flowering time in *Arabidopsis thaliana*. *Nature* **419**, 74-77 (2002).
67. J. W. Yu *et al.*, COP1 and ELF3 control circadian function and photoperiodic flowering by regulating GI stability. *Mol. Cell* **32**, 617-630 (2008).
68. Y. He, M. R. Doyle, R. M. Amasino, PAF1-complex-mediated histone methylation of *FLOWERING LOCUS C* chromatin is required for the vernalization-responsive, winter-annual habit in Arabidopsis. *Genes Dev.* **18**, 2774-2784 (2004).
69. C. Brandoli, C. Petri, M. Egea-Cortines, J. Weiss, Gigantea: uncovering new functions in flower development. *Genes* **11** (2020).

70. M. Y. Chung *et al.*, Ectopic expression of miRNA172 in tomato (*Solanum lycopersicum*) reveals novel function in fruit development through regulation of an AP2 transcription factor. *BMC Plant Biol.* **20**, 283 (2020).
71. X. Liu *et al.*, The NF-YC-RGL2 module integrates GA and ABA signalling to regulate seed germination in Arabidopsis. *Nat. Comm.* **7**, 12768 (2016).
72. B. B. Aklilu, R. S. Soderquist, K. M. Culligan, Genetic analysis of the Replication Protein A large subunit family in Arabidopsis reveals unique and overlapping roles in DNA repair, meiosis and DNA replication. *Nucleic Acids Res.* **42**, 3104-3118 (2014).
73. Y. Steinbach, L. Hennig, Arabidopsis MSI1 functions in photoperiodic flowering time control. *Front. Plant Sci.* **5**, 77 (2014).
74. Y. Z. Xu *et al.*, The chloroplast triggers developmental reprogramming when *MutS HOMOLOG1* is suppressed in plants. *Plant Physiol.* **159**, 710-720 (2012).
75. S. Sarma *et al.*, *MutS-Homolog2* silencing generates tetraploid meiocytes in tomato. *Plant Direct* **2**, e00017 (2018).
76. H. Saze, T. Kakutani, Heritable epigenetic mutation of a transposon-flanked Arabidopsis gene due to lack of the chromatin-remodeling factor DDM1. *EMBO J.* **26**, 3641-3652 (2007).
77. C. Cosio *et al.*, The class III peroxidase PRX17 is a direct target of the MADS-box transcription factor AGAMOUS-LIKE15 (AGL15) and participates in lignified tissue formation. *New Phytol.* **213**, 250-263 (2017).
78. N. Ori *et al.*, Regulation of *LANCEOLATE* by miR319 is required for compound-leaf development in tomato. *Nat. Genet.* **39**, 787-791 (2007).
79. M. Pertea, D. Kim, G. M. Pertea, J. T. Leek, S. L. Salzberg, Transcript-level expression analysis of RNA-seq experiments with HISAT, StringTie and Ballgown. *Nat. Protoc.* **11**, 1650-1667 (2016).
80. S. Anders, P. T. Pyl, W. Huber, HTSeq--a Python framework to work with high-throughput sequencing data. *Bioinformatics* **31**, 166-169 (2015).
81. M. I. Love, W. Huber, S. Anders, Moderated estimation of fold change and dispersion for RNA-seq data with DESeq2. *Genome Biol.* **15**, 550 (2014).
82. M. Kanehisa, Enzyme annotation and metabolic reconstruction using KEGG. *Methods Mol. Biol.* **1611**, 135-145 (2017).
83. S. X. Ge, D. Jung, R. Yao, ShinyGO: a graphical gene-set enrichment tool for animals and plants. *Bioinformatics* **36**, 2628-2629 (2020).
84. T. Urbanová, D. Tarkowská, O. Novák, P. Hedden, M. Strnad, Analysis of gibberellins as free acids by ultra performance liquid chromatography-tandem mass spectrometry. *Talanta* **112**, 85-94 (2013).
85. D. Rittenberg, G. L. Foster, A new procedure for quantitative analysis by isotope dilution, with application to the determination of amino acids and fatty acids. *J. Biol. Chem.* **133**, 737-744 (1940).
86. C. Pagliarani *et al.*, The accumulation of miRNAs differentially modulated by drought stress is affected by grafting in grapevine. *Plant Physiol.* **173**, 2180-2195 (2017).
87. C. Everaert *et al.*, Benchmarking of RNA-sequencing analysis workflows using whole-transcriptome RT-qPCR expression data. *Sci. Rep.* **7**, 1559 (2017).
88. J. H. Zar, Spearman Rank Correlation: Overview. *Wiley StatsRef: Statistics Reference Online* https://doi.org/10.1002/9781118445112.stat05964 (2014).
89. J. López-Ráez *et al.*, Does abscisic acid affect strigolactone biosynthesis? *New Phytol.* **187**, 343-354 (2010).
90. G. F. Ferreira e Silva *et al.*, MicroRNA156-targeted SPL/SBP box transcription factors regulate tomato ovary and fruit development. *Plant J.* **78**, 604-618 (2014).

91. S. Habib, M. Waseem, N. Li, L. Yang, Z. Li, Overexpression of *SlGRAS7* affects multiple behaviors leading to confer abiotic stresses tolerance and impacts gibberellin and auxin signaling in tomato. *Int. J. Genomics* **2019**, 4051981 (2019).
92. M. Digilio *et al.*, Molecular and chemical mechanisms involved in aphid resistance in cultivated tomato. *New Phytol.* **187**, 1089-1101 (2010).
93. M. Bemer *et al.*, The tomato FRUITFULL homologs TDR4/FUL1 and MBP7/FUL2 regulate ethylene-independent aspects of fruit ripening. *Plant Cell* **24**, 4437-4451 (2012).
94. Y. Chen *et al.*, Overexpression of bHLH95, a basic helix–loop–helix transcription factor family member, impacts trichome formation via regulating gibberellin biosynthesis in tomato *J. Exp. Bot.* **71**, 3450–3462 (2020).
95. S. Matsuo, K. Nanya, S. Imanishi, I. Honda, E. Goto, Effects of blue and red lights on gibberellin metabolism in tomato seedlings. *Hort. J.* **88**, 76-82 (2019).
96. C. Chen *et al.*, Real-time quantification of microRNAs by stem–loop RT–PCR *Nucleic Acids Res.* **33**, e179 (2005).
97. A. Zanca *et al.*, Identification and expression analysis of microRNAs and targets in the biofuel crop sugarcane. *BMC Plant Biol.* **10**, 260 (2010).